Rossby waves in the Southeast Pacific Ocean: Seasonal and interannual model-data Intercomparison

Vega, A.[1], Y. duPenhoat[1], B. Dewitte[1], O. Pizarro[2] and R. Abarca del Rio[3]

[1] Laboratoires d 'Etudes en Geophysique et Oceanographie Spatiales, Toulouse, France

[2] Programa Regional de Oceanografia Fisica y Clima, Concepcion, Chile

[3] Spaceflight Dynamics Department, CISI / CNES, Toulouse, France

e-mail: andres.vega@cnes.fr

Abstract - We investigate the variability in the Southeastern Pacific sector from altimetric and in situ data and simple model simulations for the 1995-2000 period. Whereas the low frequency variability near the coast of Chile is strongly modulated by coastal Kelvin waves remotely forced in the equatorial region, the off-shore region is characterized by coherent Rossby wave propagations at seasonal and interanual timescales, related with seasonal variability of local conditions and El Niño events, respectivelly. Sea level anomalies observed by altimetry data are shown to propagate close to theoretical linear Rossby wave speed. In order to further investigate the origin of these waves, a simple reduced-gravity linear model is used. This model requires both the wind forcing through Ekman pumping and the initial conditions at the eastern boundary. The latters are taken from a high-resolution eastern boundary linear model forced with observations and equatorial model outputs. Sensitivity tests to both the imposed Rossby wave phase speed and the boundary conditions at the Chilean coast indicate that these Rossby waves strongly depends on the initial conditions of stratification at the coast. The results show high energy of the fluxes in the coastal Humboldt current associated with the Rossby waves propagation and a dynamic strongly related with the equatorial processes.

Introduction - The seasonal and interannual variability between 1995 and 1999 of sea level anomaly (SLA), wind stress (WS) and sea surface temperature (SST) in the Southeast Pacific are investigated using satellite and tide gauges data. The focus of the present study is the interaction between the westward propagation of baroclinic Rossby waves at mid-latitude with seasonal and interannual equatorial dynamics . Coastal trapped waves (CTW), resulting from Kelvin Waves forced at the Equator, propagate southward along the Peruvian and Chilean coast with a 50-day period (Shaffer et al., 1997). These CTWs have a strong influence in the upwelling amplitude and characteristics near the coast (Vega et al., 2000). They are also likely to modulate the generation of baroclinic Rossby waves, propagating Equatorial signals in the open ocean at mid-latitudes.

Data - The data analysed correspond to the period April 1995 - December 1999 within a box bounded by 10°S–41°S, 120°W–65°W. Sea level anomalies were computed combining TOPEX/Poseidon and ERS altimeters (TP/ERS; Ducet & al, 2000). Wind stress is from ERS satellites provided by CERSAT, Brest. Sea level data from tide gauges were obtained from TOGA Sea Level Center.

Positive sea level anomalies started in early 1997 associated with a regular southward geostrophic circulation *(Fig. 1)* due to the 1997-98 El Niño (positive SST anomaly of the order of 5 °C). Total variance of low-passed SLA shows a maximun amplitude at the coast around 12°S. Large variance is also observed in open the ocean north of 20°S and south of 30°S . Similar characteristics are observed on SST variance. The maximum variance in wind stress is located at 40 °S, with larger amplitude for the zonal componant (*Figs.2*). SST and SLA patterns during the1997-98 El Niño and the later La Niña are observed on *Fig.3.* In December 1997 warm water flowed along the South American coast and a positive SLA was present near the coast up to 40°S. In December 1998, a cold period associated with La

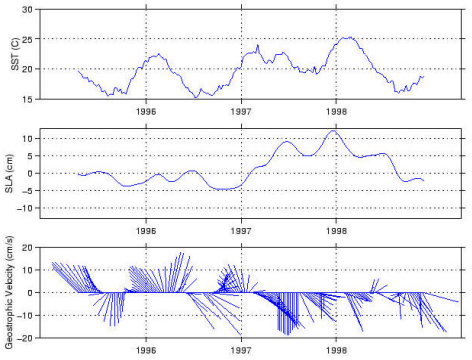

Figure 1 : Times series of SST, SLA and geostrophic velocities near the coast at 15 °S – 75 °W.

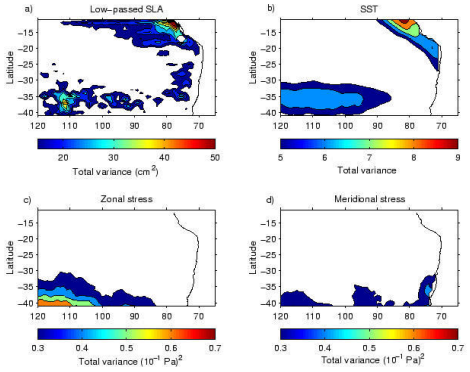

Figure 2 : Total variance of low-passed SLA, SST, zonal stress and meridional stress from April 1995 to December 1999. The SLA was filtered in space with a decorrelation ratio of 50 km and in time with half amplitude point of 30 days

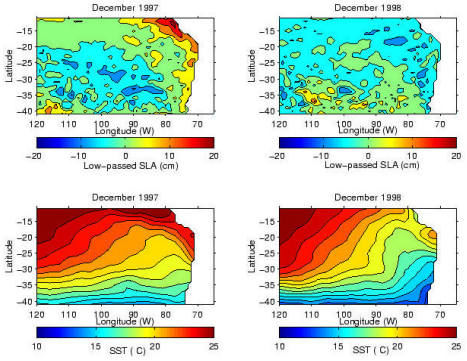

Figure 3 : Low-passed SLA and SST maps for December 1997 (El Niño event) and December 1998 (La Niña event).

Seasonal and interannual variability - The dominant annual signal of zonal stress is located in the open ocean around 30 °S, related to the high variability in the north-south displacement of the middle-latitude southern westerly winds (*Fig.4a*). The meridional stress annual signal harmonic dominates at the coastal boundary, consistent with upwelling favorable winds along the coast of Peru and Chile with an intensification in spring-summer (*Fig.4c*). The two components of the semi-annual signal are less energetic than for annual signal (*Fig.4 b,d*).

The Extended EOF analysis of TOPEX data exhibits 2 distinct modes of variability: The first and second modes are associated to the 1997 El Niño event with a large amplitude near the equator and along the coast. The third and fourth modes form a pair indicative of a propagating signal at the annual or/and semi-annual period (*Fig.5*). For these latter modes, a band of large variability extends from the central eastern Pacific at low latitude to near the coast at higher latitudes and become narrower with increasing latitude suggesting that they are associated to Rossby wave propagation from the coast (*Fig.6*).

CTWs systematically modulate coastal sea level. The sea level rose during the 1992 and 1997-1998 of El Niño (*Fig.8a*). The propagation of CTWs is evidenced in *Fig.7b* and *Fig.7*c. The poleward propagation speed is of the order of 250 km.d^{-1}, consistent with Shaffer et al.(1997). There is a low-frequency relationship between SLA at the coast from tide gauge measurements and SLA at 1000 km offshore as measured by TP/ERS (*Fig.8*; westward propagation is indicated by dashed lines). The propagation speed value, of the order of 10 km.d^{-1}, is coherent with the zonal phase speed of the observed baroclinic Rossby waves (*Fig.9*). Estimated phase speeds from TP/ERS are in close agreement with the linear theory.

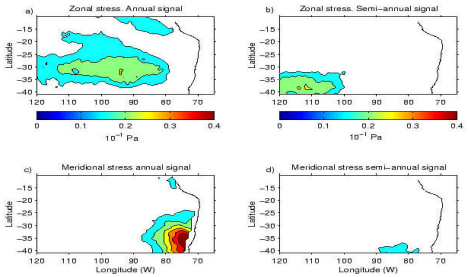

Figure 4 : Wind stress signal:. a) Zonal component annual amplitude, b) zonal component semi-annual amplitude, c) meridional component annual amplitude and d) meridional component semi-annual amplitude. Contours smaller than 0.015 Pa have been removed.

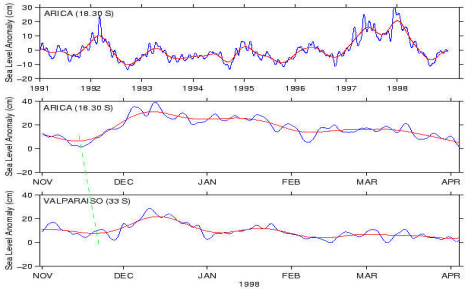

Figure 7 : Low-passed sea level from Arica (1991 to 1999) and from Arica and Valparaiso during El Nino (Nov 1997 to Apr 1998). Dashed line shows the propagation of the CTWs with a poleward speed of the order of 250 km.d^{-1}

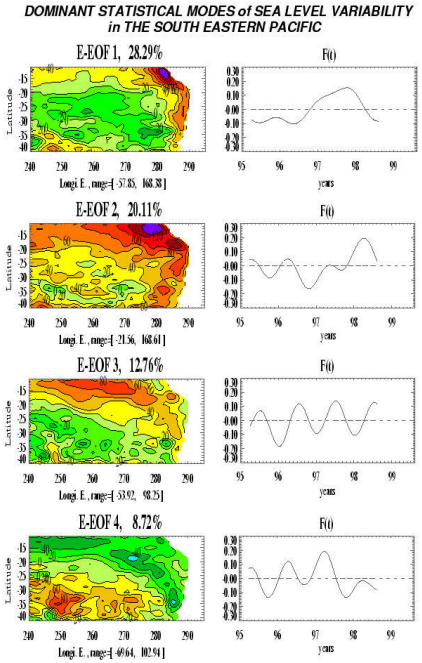

Figure 5 : Four first leading E-EOF (Extended EOF) of sea level anomalies from TOPEX. Left panels show the spatial structures of the modes and the right panels the associated time series. We use a time window of 1 yr with a 1 month interval (time resolution is 10 days). This lead to a $3*12*N_x*N_y$-dimensional "observation" vector where N_x and N_y are the numbers of longitude and latitude grid points respectively (N_x=56, N_y=31). The variance maximization procedure for these extended vectors leads to the diagonalization and eigenvalue problem of the lagged-covariance matrix. This often produces pairs of modes with similar spatial structure and explained variance but with a quadrature phase shift. The similar characteristics imply that these modes essentially describe the same propagating phenomenon. Modes which are not paired often correspond to non propagating phenomena. For example, here, modes 3 and 4 appear clearly as a pair. Maximum correlation between the associated time series is 0.92 at lag=3 months. Percentage of explained variance are indicated on top of each panels. Multiplying the time series with the amplitude of the spatial structure provide the value in mm for sea level for the corresponding mode. Contour interval is20 unit.

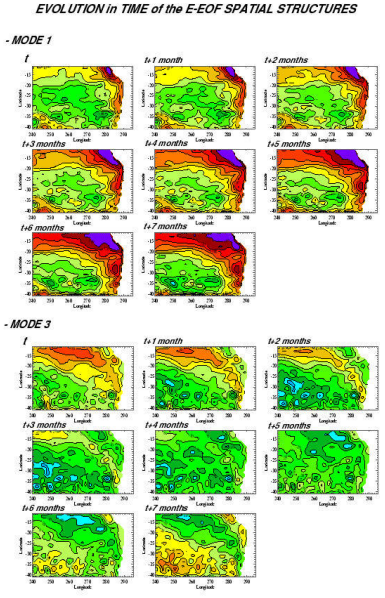

Figure 6 : Spatio-temporal evolution of the E-EOF mode 1 (top) and 3 (bottom). The maps are separated in time by 1 month. To get mm of sea level, amplitude must be multiply by a factor of about 0.2 (cf. associated time series in Fig. 5)

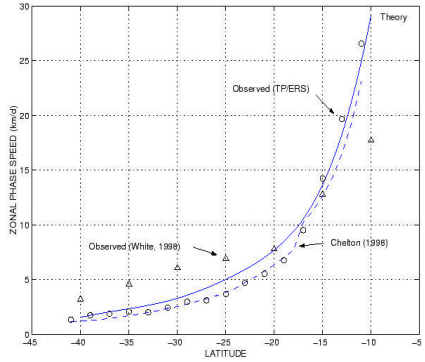

Figure 9. : Rossby wave zonal phase speed for our region, deduced from TP/ERS (circle), from theory (full line), and from Chelton (dotted line) and from White (diamonds).

Model results - Following Birol and Morrow (2000), we used a simple model vorticity equation:

$$h_t + ch_x = \frac{1}{rf} curl\,\tau(x,t) + h_b$$

with h the thermocline depth anomaly, c the non dispersive phase speed for Rossby wave at a given latitude, τ the wind stress and h_b the thermocline at the coast.

Figs. 11 and *12* show longitude/time plots at 12°S and 25°S of thermocline depth anomalies from the model forced by wind curl alone (*Hw*), and forced by wind + coastal boundary conditions (*Hwc*). Observed TP/ERS SLA (*Hsla*) are also displayed.

Hsla at 12°S shows an annual signal between 1995 and the end of 1999, except for the 1997-1998 El Niño period when *Hsla* was always negative. At 25°S, the annual signal is less clear with a large variability for lower periods. At both latitudes, *Hw* represents less than 5 % of the observed variance while *Hwc* has similar variance than the observed variance. *Hwc* variability is related to interannual variability of the thermocline depth, especially during the El Niño event. It represents the same order of amplitude. However, the annual signal is badly represented offshore. The model is highly sensitive to the coastal boundary conditions which have not been yet tuned to the observed coastal conditions.

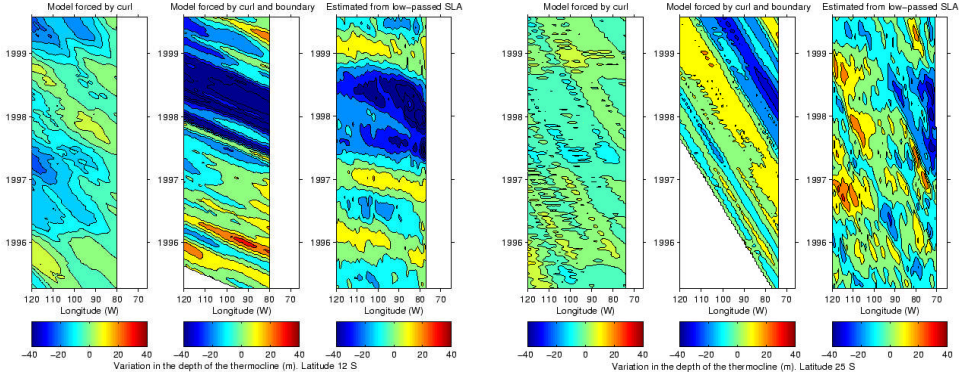

Figures 10 and 11 : Longitude-time plot at 12 °S and 25 °S of modeled thermocline depth anomalies (a) forced by wind curl, (b) forced by wind curl and boundary conditions and (c) thermocline depth anomalies from TP/ERS SLA. ERS-1/2 wind stress curl was calculated from low-passed stress components (e-folding space of 400 km and time of 30 days. Boundary conditions correspond to thermocline depth anomalies along South American coast between 10 °S and 40 °S. They are given by a high-resolution Eastern Boundary linear Model (EBM) forced by alongshore-current and sea level data (Pizarro et al., 1999). EBM was initialized at the northern boundary with the output of a Equatorial linear model forced with ERS-1/2 winds from Apr 1992 until Dec 1999 and provide realistic Kelvin wave amplitude at eastern coast (Delcroix et al., 2000).

Concluding remarks - El Niño and La Niña events are clearly observed in TP/ERS data up to 40°S: Positive anomalies of sea level near the coast were maintained for more than one year, with a southward and westward decrease in amplitude. A southward geostrophic circulation along the coast was associated with the 1997-98 El Niño. SLA maximum variability was associated with large SST variance with however different wind stress pattern characteristics. Annual SLA dominates in the coastal regions around 15 °S and in the open ocean region around 37 °S. Significant semi-annual variability exists offshore around 37°S.

Observations from altimetric data and tide gauge data indicate a westward propagation of coastal boundary features at mid-latitude, with phase speed close to the Rossby phase speed. The observed RW phase speeds are very close to theory.

Linear model results indicate that wind stress alone cannot explain low frequency variability away from the coast. They suggest that the open ocean variability is mainly forced by conditions prevailing along the South American coast. These conditions are mainly controlled by equatorial variability via propagation along the coast.

References

Birol, F. and R. Morrow (2000) Source of baroclinic waves in the Southeast Indian ocean. *J. Geophys. Res* . In press.

Chelton, D. et al. (1998) Geographical variability of the first baroclinic Rossby wave Radius of deformation. *J. Phys. Oceanogr* ., 28, 433-446.

Delcroix, T. et al. (2000) Equatorial waves and warm pool displacements during the 1992-1998 ENSO events. *J. Geophys. Res*, In press.

Ducet, N. et al. (2000) Global high resolution mapping of ocean circulation from TOPEX/POSEIDON and ERS-1/2. *J. Geophys.* Res. In press.

Pizarro, O., A. Clarke and S. Van Gorder (2000) El Nino sea level and currents along the South American coast : comparison of observations with theory. *J. Phys. Oceanogr* ., in press.

Shaffer, G. et al. (1997) Circulation and low-frequency variability near the chilean coast : remotely forced fluctuations during the 1991-1992 El Nino. *J. Phys. Oceanogr* ., 27, 217-235.

Vega, A. et al. (2000) Local and remote forcing of coastal upwelling near Valparaiso, Chile (33°S) in late spring of 1996 (La Nina) and 1997 (El Nino). Manuscript in prep.